International Conference on Mathematics, Computational Methods & Reactor Physics (M&C 2009)
Saratoga Springs, New York, May 3-7, 2009, on CD-ROM, American Nuclear Society, LaGrange Park, IL (2009)

An Analysis of Moment Preserving Methods for High Energy Ion Transport

Paul H. Smith and Anil K. Prinja
University of New Mexico
Department of Chemical and Nuclear Engineering
Albuquerque, NM 87131
phsmith@unm.edu; prinja@unm.edu

ABSTRACT

The transport of high energy ions, i.e. protons and heavier charge particles, can be a difficult and expensive calculation due to a very highly peaked DCS. We give an analysis of the most commonly used methods for approximating the scattering DCS and demonstrate the failure of these methods. In particular, we given numerical evidence that the well know Gaussian formulation breaks down for length scales that are not $O(\lambda_{tr})$. We also show that the usual moment preserving models break down due to the highly peaked nature of the transport of these particles. Due to these failures, we suggest the use of a hybrid moment preserving model for these problems. The properties of this model are briefly discussed and numerical evidence of its accuracy is given.

Key Words: high energy, protons, ions

1. INTRODUCTION

Simulating the transport of energetic charged particles is an important topic in many fields but especially in the development of radiation therapies in medical physics. Of particular interest is the calculation of the three dimensional dose distribution in human tissue resulting from an initially collimated beam of energetic electrons, protons and/or heavier ions as well as exotic subnuclear particles such as pions. The challenge is to do so in a computationally efficient manner while accounting for complex spatial heterogeneities and secondary particle emission including Bremmstrahlung and excitation radiation.

While significant effort has been devoted to refining the classical condensed history algorithm for electrons [1–3] and novel moment-preserving single event simulation schemes have recently been developed and demonstrated also for electrons [4–7], comparatively little effort has been spent on similarly increasing the fidelity of proton and heavy ion transport computations. Heavy particle condensed history codes such as MCNPX rely largely on the Fermi model presented by Rossi [8] to sample angular deflections at the step boundaries and the Vavilov straggling model [9] to sample energy losses. These are known to provide inadequate accuracy and are particularly suspect at material interfaces.

The goal of this work is to develop and demonstrate moment-preserving models for proton and heavier particle transport. Preliminary work has shown that the higher mass and charge of such particles in some ways presents a greater computational challenge to these methods than do electrons. Particular emphasis will be placed on the identification of the additional difficulties and how they may be overcome.

2. High Energy Ion Transport Physics

Charged particle transport simulations are computationally very slow due primarily to small mean free paths and differential cross sections that are extremely peaked at small energy losses and small scattering angles. This singular behavior is suggestive of a process in which a particle interacts very often but the result of most of these interactions is to leave the particle with nearly the same energy and direction vector. In these cases, it is not the result of each interaction that is of importance but of the average behavior of an ensemble of particles over many mean free paths.

All of the analog transport methods in common use simulate collisions based on the true mean free path given by the physics of the problem. This can be very expensive when the scattering process has a very small mean free path. The essence of moment-preserving approaches is to define mean free paths and pseudo-differential cross sections that are representative of the average behavior after a large number of true collisions. This is comparable to a condensed history technique where multiple scattering distributions are used to sample a particle's state after large, fixed steps. The difference, however, is that collisions occur as independent, uncorrelated events much like they do in a true physical setting. This removes many of the issues that arise at interfaces and boundaries with condensed history. We also show later that the physics can be more accurately modeled over reasonable length scales with moment preserving methods as opposed to some of the simple models that are in use still today.

There are two important processes that need to be treated in high energy ion transport, elastic scattering off atomic nuclei and inelastic collisions with atomic electrons. Typically most of the energy loss occurs in inelastic events resulting from collisions with electrons where angular changes are considered negligible. On the other hand, elastic scattering off nuclei contributes to most of the angular spreading while energy loss due to these events is negligible. Under these conditions, the transport process is described by the Boltzmann transport equation:

$$\begin{aligned}\Omega \cdot \nabla \psi(\mathbf{r}, \Omega, E) = &\int_{4\pi} \sigma_n(\mathbf{r}, \Omega \cdot \Omega', E)\psi(\mathbf{r}, \Omega', E)d\Omega' - \sigma_{n,t}\psi(\mathbf{r}, \Omega, E) \\ &+ \int_{Q_{min}}^{Q_{max}} \sigma_e(\mathbf{r}, \Omega, E' \rightarrow E)\psi(\mathbf{r}, \Omega, E')dE' - \sigma_{e,t}\psi(\mathbf{r}, \Omega, E) \end{aligned} \quad (1)$$

The boundary condition for a narrow monoenergetic beam can be given by,

$$\psi(\mathbf{r}_b, \Omega, E) = \delta(\mathbf{r} - \mathbf{r}_b)\delta(E - E_0)\delta(\Omega - \Omega_0) \quad (2)$$

Moment preserving methods for inelastic scattering have been successfully demonstrated for both electrons [6] and protons. Results for proton inelastic scattering will be given later in this paper. The success of these methods over such a wide range of particles for inelastic scattering naturally suggests that they should also work well for elastic scattering over the same range of particles because the differential cross sections are mathematically very similar. For inelastic collisions

with atomic number Z_1 bombarding a target with atomic number Z_2, the DCS takes the form,

$$\sigma_e(E,Q) = 2\pi Z_1^2 Z_2 \rho \frac{r_e^2 m_e c^2}{\beta^2 Q^2}\left(1-\beta^2\frac{Q}{Q_{max}}\right), \quad Q_{min} < Q < Q_{max} \tag{3}$$

Here, Q is the energy lost by the incident particle, ρ is the atomic density of the material, and $\beta = v/c$ for the incident particle. We also note that Q_{min} is a cutoff energy that is usually chosen to be greater than the ionization energy of the target atoms. The resulting total cross section is very large, but the moments of the cross section defined by

$$Q_n(E) = \int_{Q_{min}}^{Q_{max}} Q^n \sigma_e(E,Q)dQ \tag{4}$$

are much smaller in comparison. Since Q_1 is just the stopping power and Q_2 is the straggling coefficient, then we also have a physical interpretation for the first two moments. These moments serve as the basis for the moment preserving methods described later.

For elastic scattering, the DCS for the same problem is well approximated by the screened Rutherford DCS given by

$$\sigma_n(\mu_0,E) = \frac{K(E)}{(1+2\eta(E)-\mu_0)^2}, \tag{5}$$

Here $\mu_0 = \Omega\cdot\Omega'$ is the cosine of the scattering angle. The energy dependent constants $K(E)$ and $\eta(E)$ take a different form for different particle types. The constant η is known as the screening parameter and is the only thing keeping the DCS from being singular at $\mu_0 = 1$, a value corresponding to no deflection. Formulas for the values of these constants can be found in the literature [8]. Figure 1 shows the value of these parameters for electrons, protons, and alphas on tungsten as a function of the unitless parameter $\tau = E/m_0c^2$ where m_0 is the rest mass of the incident particle. The screening parameter gives an indication of the magnitude of the mean

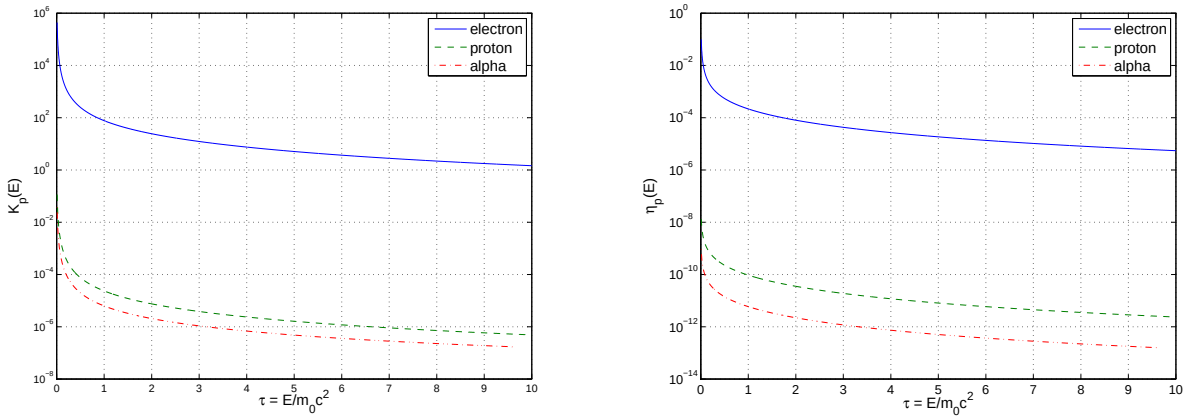

Figure 1. Dependence of the screened Rutherford DCS parameters $K_p(E)$ (left) and $\eta_p(E)$ (right) as a function of $\tau = E/m_oc^2$ for electrons, protons, and alphas on tungsten

cosine of scattering given by

$$\bar{\mu} \approx 1 - 2\eta \ln\left(\frac{1}{\eta}\right) \tag{6}$$

From this we see that high energy ion scattering is much more forward peaked then electron scattering. As a result, we find that the momentum transfer moments of the DCS given by

$$\sigma_{k,p}(E) = \int_{-1}^{1} (1-\mu)^k \sigma_{n,p}(\mu, E) d\mu \tag{7}$$

tend to get smaller for heavier incident particles. However, the value of $K_p(E)$ is much larger for electrons than it is for heavier ions. Consequently, there tends to be a cancellation effect in the total cross section, given by

$$\sigma_{t,p} = \frac{K_p(E)}{2\eta(\eta+1)} \tag{8}$$

That is, we see a small variation in the total cross section at a fixed τ for different particle types. Figure 2 shows the total cross section and the first moment of the cross section generated from the relativistic Rutherford elastic scattering DCS using the parameters given in Fig. 1.

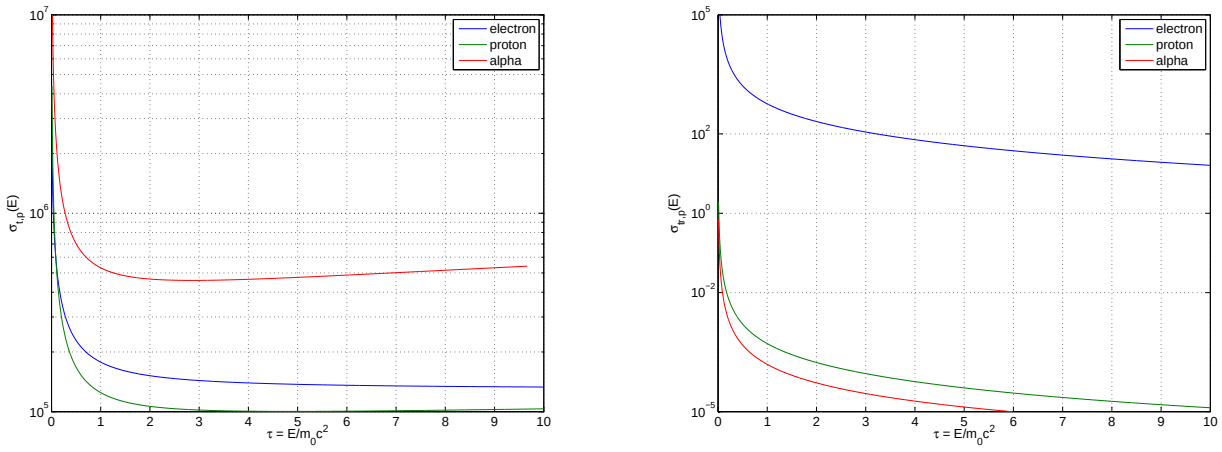

Figure 2. Dependence of the screened Rutherford total cross section(left) and the first moment of the cross section (right) as a function of $\tau = E/m_o c^2$ for electrons, protons, and alphas on tungsten

The analogy between inelastic and elastic scattering DCS becomes clear if we make the correspondance $(1 + 2\eta - \mu) \rightarrow Q$. The result is that we get nearly identical forms for the DCS, but the value that correpsonds to Q_{min} for the elastic cross section is 2η. We can see from the values of η given in figure 1 that 2η can be much smaller than an ionization energy, which is the lower limit for Q_{min} for the inelastic DCS. In the language of charged particle transport, we can say that heavy ion elastic scattering looks like the simulation of individual soft collisions for inelastic scattering. This fact embodies the difficulty of using moment preserving methods for simulating elastic scattering of heavy charged particles.

3. Approximations for Forward Peaked Transport Processes

The Fokker Plank approximation is a popular and widely applied approximation for simulating highly peaked transport physics. It can be derived from the transport equation rigorously in the limit $\sigma_{t,e} \rightarrow \infty$ and $\bar{\mu} \rightarrow 1$ such that σ_{tr} remains finite. In this limit, the elastic scattering operator on the right-hand side of Eq.(1) can be replaced by a spherical Laplacian operator on the unit sphere.

$$\Omega \cdot \nabla \psi(\mathbf{r}, \Omega, E) = \frac{\sigma_{tr}}{2} \left(\frac{\partial}{\partial \mu}(1-\mu^2)\frac{\partial}{\partial \mu}\psi(\mathbf{r}, \Omega, E) + \frac{1}{(1-\mu)^2}\frac{\partial^2}{\partial \phi^2}\psi(\mathbf{r}, \Omega, E) \right) \tag{9}$$

This is a very convenient approximation for deterministic transport methods, but it is not so for Monte Carlo methods. However, the Fokker Planck operator can itself be approximated using the asymptotic equivalence

$$\frac{\sigma_{tr}}{2}\nabla^2_{\Omega}\psi(\mathbf{r}, \Omega, E) = \lim_{\hat{\mu}\rightarrow 1} \frac{\sigma_{tr}}{1-\hat{\mu}} \int_{-1}^{1} \delta(\mu_0 - \hat{\mu})\psi(\mathbf{r}, \Omega, E) d\mu_0 \tag{10}$$

With this approximation, we can simulate a FP approximation using Monte Carlo methods by simply choosing $\hat{\mu}$ close enough to 1 such that the result of the simulation no longer changes with further increasing $\hat{\mu}$. We will show later that this approximation is equivalent to a one moment discrete model in the moment preserving framework.

The FP approximation has been shown by Börgers and Larsen to perform poorly for relativistic Rutherford scattering problems and more generally for DCS's with a large scattering angle tail that varies as $1/(1-\mu)^2$ [10]. In that paper, they were able to isolate the error term for a FP approximation and show that it is $O(\text{var}(\mu_0)/(1-\bar{\mu}_0))$. For the relativistic Rutherford DCS, this yields

$$\frac{\text{var}(\mu_0)}{1-\bar{\mu}_0} = \frac{2}{\ln(1/(1-\bar{\mu}_0))} + O\left(\frac{1}{\ln(1/(1-\bar{\mu}_0))}\right) \tag{11}$$

The problem is that this error tends toward zero only logarithmically with the average scattering angle. Figure 3 shows the slow reduction of the leading order term of the error for a Fokker Planck approximation to the relativistic Rutherford DCS. We note that the range of $1-\bar{\mu}_0$ for high energy protons in many applications is $10^{-10} - 10^{-8}$, and it is much larger still for applications with high energy electrons.

Using Fokker-Planck to approximate the entire scattering kernel is generally considered to be inaccurate. The object of the Boltzmann Fokker Planck approximation is to simulate the large angle tail exactly while approximating the peaked part with the FP approximation. This works in a Monte Carlo simulation by choosing a cutoff deflection cosine, μ^*, using Eq.(10) to simulate the peaked portion ($\mu > \mu^*$), and sampling the large angle tail ($\mu < \mu^*$), an appropriate fraction of the time. This method is given formally by the approximation

$$\Omega \cdot \nabla \psi(\mathbf{r}, \Omega, E) = \int_{4\pi} \sigma^*_n(\mathbf{r}, \mu_0, E)\psi(\mathbf{r}, \Omega', E) d\Omega' - \sigma^*_{n,t}\psi(\mathbf{r}, \Omega, E) + \frac{\sigma^*_{tr}}{2}\nabla^2_{\Omega}\psi(\mathbf{r}, \Omega, E) \tag{12}$$

with the approximate DCS

$$\sigma^*_n(\mathbf{r}, \mu_0, E) = \begin{cases} K_p(\mathbf{r}, E)/(1 + 2\eta_p(\mathbf{r}, E) - \mu_0)^2 & -1 \leq \mu_0 < \mu^* \\ 0 & \mu^* \leq \mu_0 \leq 1 \end{cases} \tag{13}$$

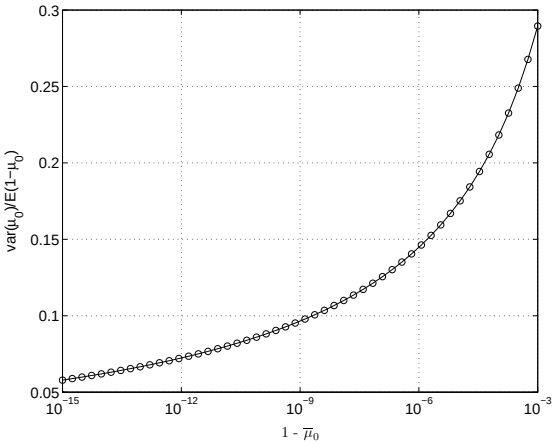

Figure 3. Magnitude of the leading order error term in the FP approximation for varying values of $1 - \bar{\mu}_0$.

and the total cross section $\sigma^*_{n,t}$ obtained by integrating Eq.(13) over all μ_0. The quantity σ^*_{tr} is given by integrating the Rutherford DCS over the interval from μ^* to 1.

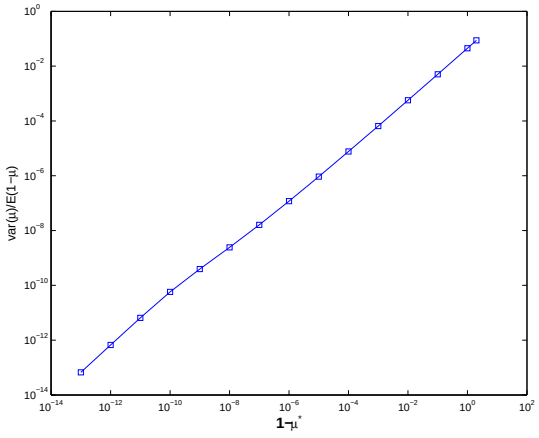

Figure 4. Magnitude of the leading order error term in the FP approximation of the peaked part of the DCS for 1700 MeV protons incident on tungsten metal with varying values of $1 - \bar{\mu}^*$

The reason for the effectiveness of the BFP method can be found by considering Fig. 4. Here we see the leading order error term for the Fokker-Planck approximation of the Rutherford DCS for 1700 MeV protons on tungsten metal as a function of $1 - \mu^*$. It appears that the accuracy is nearly first order in $1 - \mu^*$ when approximating only the portion of the DCS with $\mu > \mu^*$. The caveat is that we still must choose a cutoff very close to 1, leaving us to simulate a large portion

of the DCS exactly.

As mentioned earlier, a popular method for simulating charged particle transport processes is the condensed history method. In this method, a particle is moved through a fixed step and the state of the particle is retrieved by sampling a multiple scattering angular deflection and energy loss from predetermined distributions. Different distributions are used for different particles, but the most prevelant distribution for heavy ions comes from the Fermi approximation of the FP operator. The Fermi approximation is derived from Eq.(9) by assuming $\mu_0 \approx 1$. We may then approximate the spherical Laplacian with a planar Laplacian to obtain

$$\frac{\partial \psi}{\partial z} + \eta \frac{\partial \psi}{\partial x} + \xi \frac{\partial \psi}{\partial y} = \frac{\sigma_{tr}}{2} \left(\frac{\partial^2 \psi}{\partial \eta^2} + \frac{\partial^2 \psi}{\partial \xi^2} \right), \quad -\infty < \eta, \xi < \infty \tag{14}$$

The solution to this equation can be found analytically and is given by a Gaussian in space and angle. We see that this solution can never be better than the solution to the FP approximation to the transport equation. However, it is thought that this approximation is no worse in cases where scattering is very forward peaked. For a more detailed discussion, the reader is referred to Börger's paper [10].

Figure 5 shows the distributions obtained when using the Fokker-Planck and Fermi equations to approximate the Rutherford cross section for the problem of 1700 MeV protons incident on tungsten metal. The results are overlaid with the a result obtained by an analog Monte Carlo method. Based on the previous discussion, it is no surprise to see that the Fermi result is indeed as good as the Fokker-Planck result. However, the discrepancy between these approximations and the analog result is very large, even though the scattering is very forward peaked. The

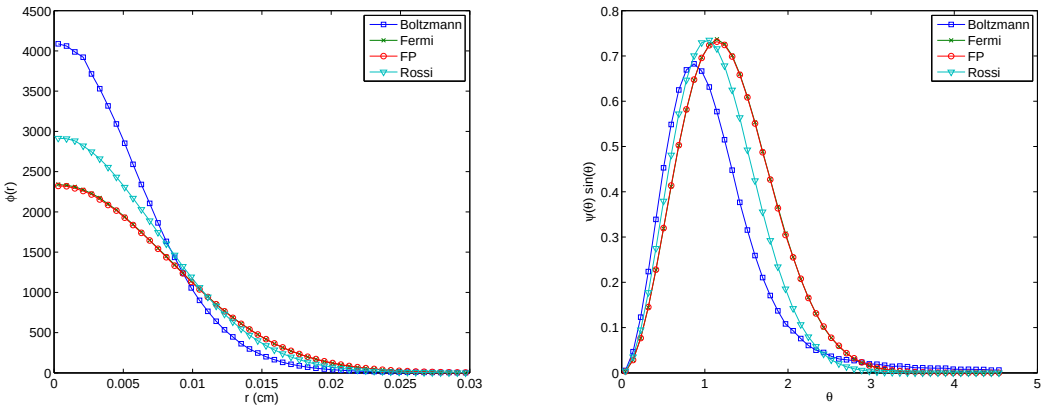

Figure 5. Distribution of particles from centerline of beam (left) and angular distributions (right) for the Fokker Planck approximation, Fermi Approximation, and a correction to the Fermi approximation due to Rossi.

approximation used in MCNPX is a Gaussian with a modified variance as given by Rossi [11]. One can show that the parameter used to set the variance of the Gaussian by Rossi is the same as that obtained by just approximating the Fokker-Planck equation if one sets an upper bound of $\theta_2 = 1$ radian to the validity of the approximation. However, a correction is proposed for $\theta_2 < 1$

which amounts to the third distribution given in Fig. 5. This correction is equivalent to using a smaller value for σ_{tr} in the Fermi approximation. From this, we see that no correction for the Gaussian can correctly predict both the singular part of the DCS as well as the large angle scattering tail. The result of any attempt will still lead to a shifting of the angular spectra to higher angles since too much weight is given to large angle scattering.

This analysis leads us to believe that a moment preserving approach could help capture more details of the DCS by simply preserving more then just the first moment. In the next section, we discuss this approach and its shortcomings.

4. Moment Preserving Methods

In a rigorous manner, it can be shown that the FP operator is a leading order approximation to an unstable infinite expansion. In this expansion, the moments given by Eq.(4) and Eq.(7) become the important parameter in the expansions of each of the scattering integrals. The FP operator simply becomes the first terms in each expansion, where higher order terms are thought to be negligible for sufficiently forward peaked transport processes. However, as we stated earlier, this approximation is only logarithmically convergent with decreasing transport cross section $\sigma_{tr} = \sigma_1$.

In our approach, a new transport equation is proposed that is equivalent to the analog equation given in Eq.(1) except with a new DCS in each integral. That is, we let σ_e^* and σ_n^* replace σ_e and σ_n in (1) where we have,

$$\begin{aligned} \sigma_e^* &= \sum_{i=1}^{N} \frac{\alpha_{e,i}}{\beta_{e,i}} \exp\left(\frac{-Q}{\beta_{n,i}}\right) \\ \sigma_n^* &= \sum_{i=1}^{N} \frac{\alpha_{n,i}}{\beta_{n,i}} \exp\left(\frac{\mu-1}{2\beta_{e,i}}\right) \end{aligned} \tag{15}$$

The parameters given by β and α are free. Thus there are $2N$ degrees of freedom for each cross section. It can be shown rigorously that the new transport equation is equivalent to a higher order Fokker-Plank expansion up to a truncation of $2N$ terms in the sum if we preserve the first $2N$ energy loss moments in Eq.(4) of the inelastic cross section and the first $2N$ generalized momentum transfer moments in Eq.(7) of the elastic cross section[7]. Furthermore, this representation is stable and it leads to larger mean free paths. Thus, we may use any numerical procedure to solve the new equation that we would use for a neutral particle equation. The model described in [7] will be referred to as the exponential model of order $M = 2N$ for the remainder of this paper. Another representation similar in spirit to the exponential model is given by,

$$\sigma_e^* = \sum_{i=1}^{N} \alpha_{i,e} \delta\left(Q - \beta_{i,e}\right) \tag{16}$$

$$\sigma_n^* = \sum_{i=1}^{N} \alpha_{i,n} \delta\left(\mu - \beta_{i,n}\right) \tag{17}$$

Again we must preserve the first $2N$ generalized moments of each cross section to obtain an asymptotically equivlent representation. This model is referred to as the discrete model of order $M = 2N$ for the remainder of this paper.

Preserving moments for either the discrete model or the exponential model of order M for either cross section leads to the following coupled set of nonlinear equations.

$$\sum_{n=1}^{N} \alpha_n \beta_n^j = C_j \sigma_j, \quad j = 1, 2, ..., M \tag{18}$$

The terms σ_j are either the energy loss or momentum transfer moments where appropriate. The factor C_j distinguishes the exponential model equations from the discrete model equations. For the discrete model, we have $C_j \equiv 1$ for all j. For the exponential model, we get $C_j = 1/j!$. In either case, we have equations similar to those found in the classical quadrature problem. These equations are notoriously ill-conditioned and require special treatment to solve for truncations higher than $M = 6$. However, analytic solutions are available for the equations with $M \leq 4$. We will present numerical examples for which the order is no larger than 4 in this paper. We note however, that though higher order truncations can be found, experience has shown that the mean free path for the renormalized cross section becomes smaller with higher order. Therefore, it is typically not advantageous to solve the higher order problems due to run times that approach those of the analog problem.

We find that these approximations can fail to give sufficient gains by some measures of accuracy. In particular, we find that preserving 4 moments for elastic scattering of heavy ions leads to mean free paths that are too large to use. To see why this is the case, we may consider the analytic solution of Eq.(18) for the exponential model of order 2 and for the case of angular deflections. We get

$$\alpha = 2\frac{\sigma_1^2}{\sigma_2}, \quad \beta = \frac{\sigma_2}{4\sigma_1} \tag{19}$$

We see that if $\sigma_1 << 1$, then σ_2 must be very small to keep the mean free path, which is equal to $1/\alpha$, from blowing up. In a sense, the moment preserving methodology seems to be working too well since a large mean free path is desired. However, if the mean free path exceeds about $1/10$th of the average length scale of the problem, then we will get artifacts from the method that are due solely to the moment preserving approximation. For instance, if we are considering 1700 MeV protons incident on tungsten metal, we would have $\sigma_1 = 2 \times 10^{-4}\text{cm}^{-1}$ and $\sigma_2 = 1.75 \times 10^{-5}\text{cm}^{-1}$ This gives $1/\alpha \approx 250$cm, but the range of protons in this problem is only about 60cm[12]. Using any method to solve this problem will fail to capture the physics since the medium will appear invisible to the protons, while the true physics leads to many collisions and substantial deflection.

One method that has been developed to take care of inadequate mean free paths for moment preserving approximations is to only preserve $M - 1$ moments and introduce the Mth equation

$$\sum_{i=1}^{N} \alpha_i = \frac{1}{\lambda^*}, \tag{20}$$

where λ^* is some user inputted mean free path. The set of equations to solve are very similar to Eq.(18) and the result is guaranteed to have a manageable mean free path. This method has been used with both $M = 4$ and $M = 6$, that is where three and five moments have been preserved, for the elastic scattering problem.

Figure 6 shows the success of the four moment approximation for the inelastic scattering problem. There we have the energy straggling for two length scales, 0.5 cm and 20 cm. In each case, the four moment exponential model results capture the straggled energy distributions well, even when a Gaussian approach fails. The two moment model has limited success in each case. We also see the artifacts that arise when the mean free path is too large for the problem with the discrete model. Finally, we see that we may use an adjustable mean free path model while preserving three moments to capture the distribution even for short length scales. From this result and many others, we can deduce that the moment preserving method is robust for approximating the inelastic scattering of heavy particles. The stopping power, σ_1, for this problem ranged from 11.3 to 11.5 MeV/cm as the penetration was small compared to the range of protons in tungsten.

Applying the same models to the elastic cross section fail to produce the same success. Figure 7 shows the angular distributions for the same geometry and physics as in Fig. 6 for 0.5 cm and 5.0 cm slabs, with $\sigma_1 = 0.0002$ with $\sigma_2 = 0.00001$. From the discussion above, we see that we cannot use a simple four moment model to approximate the cross section. Instead, we use a three moment model with $\lambda = 0.1$ cm. We also used a five moment model with the same mean free path with identical results as those shown in Fig. 7. The results tell us that moderate gains in accuracy can be made over the Fokker Planck result, but there is still much room for improvement. Furthermore, the results indicate that, like the inelastic DCS case, we can get better accuracy for deeper penetrations.

Our results seem to suggest that we need to adopt a new length scale over which our approximations are valid. The length scale should be $O(1/\sigma_1)$ in order for the moment preserving approximations to be correct. This interpretation is consistent with the success of the method with the inelastic DCS where $1/\sigma_1 \approx 1/10$ and with the poor performance of the method with the elastic cross section where $1/\sigma_1 \approx 10^{-4}$. The only way to improve the accuracy of the method is to preserve more moments, and effectively resolve the mean free path, or to use the method only for length scales that are $O(10^2) - O(10^4)$.

5. Hybrid Methods

To obtain more accurate solutions then have been shown previously, we must find a way to accurately capture the tail of the DCS while still approximating the peaked part. We start with the observation

$$1 - \mu_0 + 2\eta \approx 1 - \mu_0 \tag{21}$$

when $1 - \mu_0 >> 2\eta$. Therefore, the magnitude of the parameter η is only important where the DCS is singular. This is the part that we would like to approximate. Thus, we choose an approximate DCS given by

$$\sigma_n^*(\mu_0, E) = \frac{K_p(E)}{(1 + 2\eta_p^*(E) - \mu_0)^2} + \sum_{i=1}^{N} \frac{\alpha_{n,i}}{\beta_{n,i}} \exp\left(\frac{\mu - 1}{2\beta_{e,i}}\right) \tag{22}$$

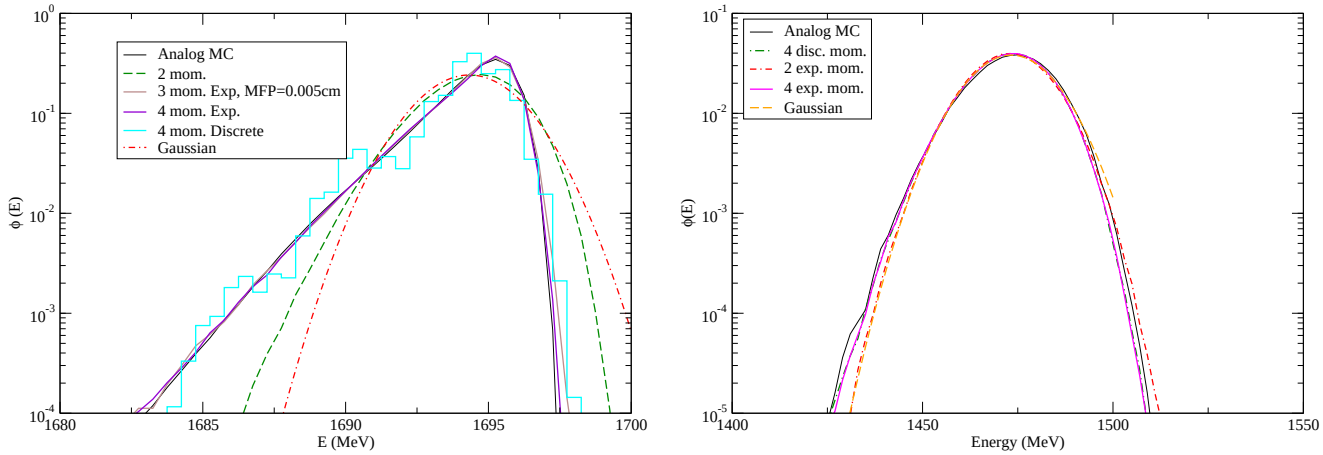

Figure 6. Straggled energy distributions for 1700 MeV protons incident on tungsten metal for 0.5 cm (left) and 20 cm (right) thick slabs. Both two and four moment approximations are shown for the exponential model, and a four moment approximation is shown for the discrete model. The Gaussian is based on an analytic solution to the straight ahead transport equation due to Fermi.

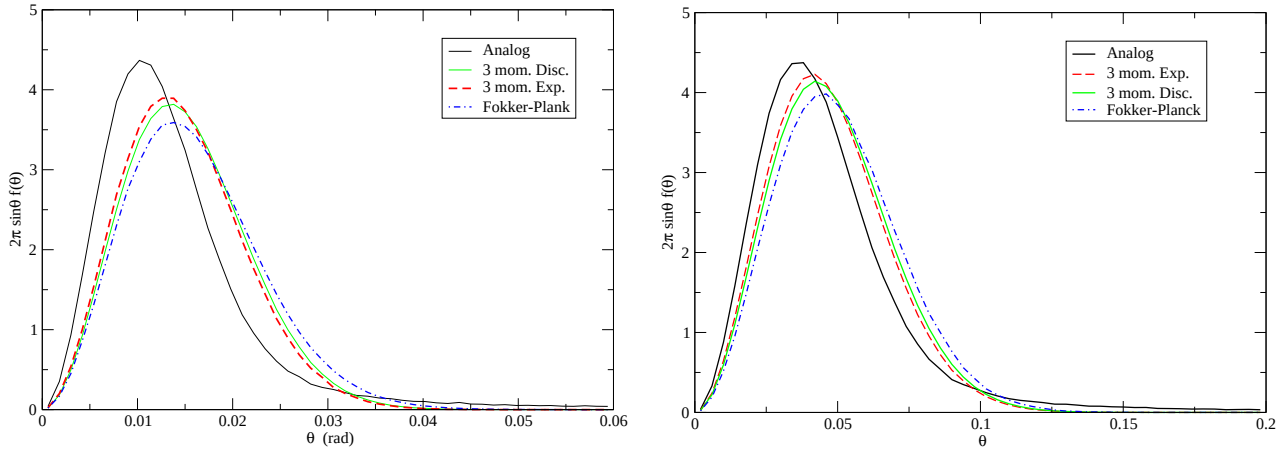

Figure 7. Angular distributions for 1700 MeV protons incident on tungsten metal for 0.5 cm (left) and 5 cm (right) thick slabs. Both three moment discrete and exponential approximations are shown along with a Fokker Planck result and an analog Monte Carlo result.

This will be known as the exponential hybrid model of order M for the remainder of this paper. Delta functions may be used in lieu of exponentials to give a discrete hybrid model of order M.

In Eq.(22), the parameter $K_p(E)$ is the same as that given by the analog DCS in Eq.(5), but the $\eta^*(E)$ is now chosen to yield a sufficiently long mean free path. This technique guarantees that the first term in $\sigma^*(\mu_0, E)$ can be made arbitrarily close to the analog cross section $\sigma(\mu_0, E)$ when $1 - \mu_0 + 2\eta^*$ is sufficiently large. The remaining terms are present to approximate the peaked part of the analog DCS. The process of choosing the α_i's and β_i's amounts to preserving moments of the residual DCS given by $\sigma_n(\mu_0, E) - \sigma_n^*(\mu_0, E)$. The nonlinear system given by Eq.(18) remains the same.

To test these methods, we use the same test problem as before, 1700 MeV protons incident on tungsten, with a slab width of 1 cm. Figure 8 shows the result obtained using an analog Monte Carlo approach, the Fokker-Planck approximation, and two discrete hybrid methods that preserves three moments with an adjustable mean free path. The mean free path was set to 0.1 cm and 0.01 cm to obtain the two results shown.

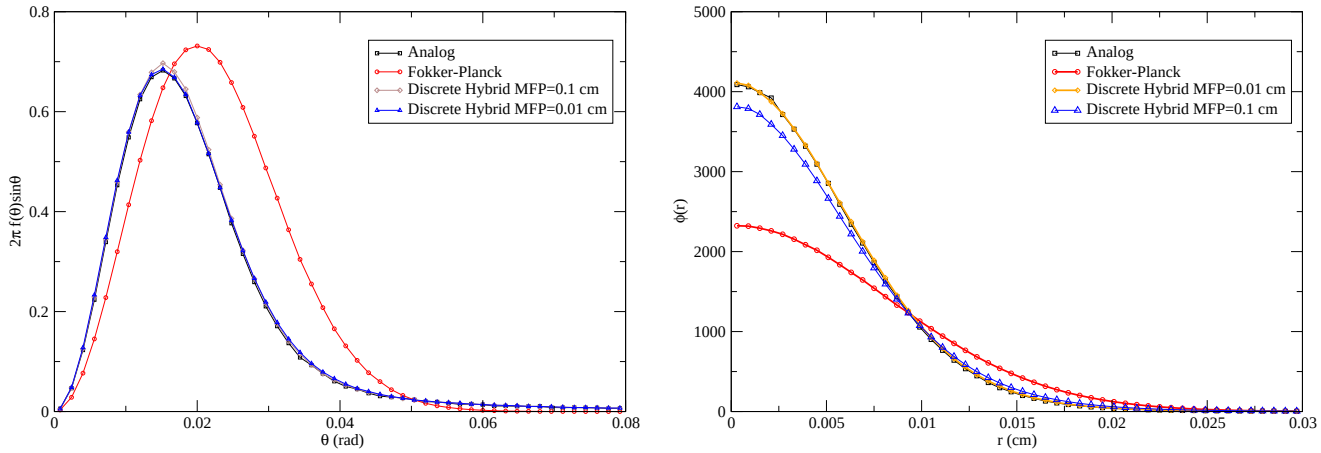

Figure 8. Angular distributions (left) and radial distributions from the center of the incident beam (right) for 1700 MeV protons incident on tungsten metal for a 1.0 cm thick slab. Included are results generated from an analog Monte Carlo simulation, a Fokker-Planck approximation, and a discrete hybrid method preserving three moments with a MFP equal to 0.1 cm and 0.01 cm

We can see from the figure that the hybrid results have the potential to capture both the peaked portion and the tail accurately while still sustaining a sizeable speedup. The success of the method can be argued with the aide of the previous discussion on the BFP approximation. The hybrid method is simply a smooth version of the BFP method since we are only using the moment preserving method to approximate the singular part of the DCS. We see from Fig. 4 that the leading order error term in a Fokker Planck approximation decreases substantially as we decrease $1 - \mu^*$. This is effectively accomplished by decreasing η^* in the hybrid method. However, since we are using a higher order method than Fokker Planck to approximate the peaked part, with the remaining moments accounted for approximately by way of the form used for the moment

preserving approach, we can actually get a smaller error term than that given by Fig. 4. To summarize, we are combining the power of a moment preserving approach with the accurate BFP method in a smooth and easily extendable way without the introduction of differential operators.

The advantage of using the approximation is easily seen from Table I. Here we compare the Monte Carlo simulation time required per 1000 particle for various methods for the problem given in Fig. 8. We list the speedup, defined as the ratio of the simulation time of the approximation to the analog simulation time, and we list the maximum relative local error in any bin for the radial distributions generated at a 1 cm thickness. Since we use identical bin structures for each simulation, this is a consistent measure of accuracy. We also note that the simulation for the analog approximation was run such that the maximum sample variance of any bin was about 1.0% and each of the approximations had less than 0.33% standard deviations in each bin.

Table I. Computing times, speedup, and max. relative errors for the problem given in Fig. 8

Model	CPU times (/1000 particles)	speedup factor	Max. loc. rel. err.
Analog MC	28.9 sec.	1.0	0%
Fokker Planck	0.028 sec.	100	48.7%
3 mom. discrete	0.029 sec.	100	24.3%
3 mom. exponential	0.031 sec.	99.9	22.1%
disc. hybrid mfp=0.01	0.030 sec.	99.9	0.13%
disc. hybrid mfp=0.10	0.003 sec.	1000	5.3%

For the first three five listed simulations, the mean free path was set to a hundredth of the mean free path of the analog cross section. Therefore, the computing times were comparable for each of the simulations. We can see that there is a dramatic gain in relative accuracy by using the hybrid model, as we are able to more accurately capture the entire DCS with this method. It is also interesting to note that there is no gain in relative accuracy for the Fokker Planck method or the basic moment preserving methods by using smaller mean free paths. We have saturated any accuracy to be gained by the methods by setting the mean free path as low as it is here. For the hybrid model, the model performs well within the statistical tolerances for this problem. By allowing the mean free path to increase by a factor of 10, we see that the method is still much more accurate than the other methods, but we get a much better speedup.

6. Conclusions and Future Work

From the above numerical evidence, it seems that we have developed a method that can give extremely large speedups while still performing much better than the best case scenario for a Fokker Planck approximation, and hence a Fermi approximation. Furthermore, the method can be tuned to a users needs. If a user decides to let the mean free path slip all the way to that of the analog DCS, then we get the exact analog DCS. On the other hand, if the user can let the mean free path approach those seen in many neutronics type calculations to get faster solutions. This freedom allows users to make the method work for their needs, which is its most attractive feature.

We have seen that the Fermi model can never be better than Fokker Planck, and we have seen that the Fokker Planck model performs very poorly for many charged particle transport applications. A simple moment preserving approach doesn't improve the accuracy of a Gaussian distribution based method as much as it does with the energy straggling DCS. Therefore, it seems that our approach provides a better means for accurately reproducing the angular and spatial spreading of a pencil beam of heavy charged particles.

We are working on combining this method with energy loss moment preserving models for deep dose calculations. We hope to show that we can more accurately reproduce a Bragg peak with our approach then with the approximations mentioned above. Interesting new challenges arise when we consider the moment preserving and hybrid methods in deep penetration problems. However, prelimary findings are that the methods still give considerable speed-ups and accuracy. Results are forthcoming.

The next step is to implement our approach into a high energy physics simulation package such as MCNPX. Here, we will be able to compare the method's speed and accuracy in the presence of more precise nuclear physics models. It is our belief that our approach will speed up the elastic and inelastic scattering collision processes in the code, and that the overall effect will be apparent, even in the presence of these models.

REFERENCES

[1] M. J. Berger, *Methods in Computational Physics*,Vol. 1, edited by B.Adler, S. Fernbach, and M. Rotenberg (Academic Press, New York, 1963).

[2] E.W. Larsen, Ann. Nucl. Energy, **19**, 701 (1992).

[3] I. Kawrakow and A.F. Bielajew, Nucl. Instrum. Methods Phys. Res. B, **142**, 253 (1998).

[4] D.R. Tolar and E.W. Larsen, Nucl. Sci. Eng., **139**, 47 (2001).

[5] C.L. Leakeas and E.W. Larsen, Nucl. Sci. Eng., **137**, 236 (2001).

[6] B.C. Franke and A.K. Prinja, Nucl. Sci. Eng., **149**, 1 (2005).

[7] A.K. Prinja and B.C. Franke, Trans. Amer. Nucl. Soc., **90**, 281 (2004)

[8] B. Rossi, *High-Energy Particles*. Prentice Hall, New York (1952).

[9] P. V. Vavilov, Soviet Physics JETP, **5**, 749 (1957).

[10] E. Larsen and C. Börgers, *Medical Physics*, **Vol. 23, No. 10**, pp.1749-1759 (1996)

[11] L. Waters, *Technical Report LA-UR-02-2607, LANL* (April 2002)

[12] J.F. Janni *Atomic Data and Nuclear Data Tables*, **Vol. 27 No. 4/5**, pp.515 (July/Sept. 1982)